© 2016. Published by The Company of Biologists Ltd | Journal of Experimental Biology (2016) 219, 1394-1404 doi:10.1242/jeb.135673

RESEARCH ARTICLE

Spatial resolving power and spectral sensitivity of the saltwater crocodile, *Crocodylus porosus*, and the freshwater crocodile, *Crocodylus johnstoni*

Nicolas Nagloo[1,2,*], Shaun P. Collin[1,2], Jan M. Hemmi[1,2] and Nathan S. Hart[1,2,3]

ABSTRACT

Crocodilians are apex amphibious predators that occupy a range of tropical habitats. In this study, we examined whether their semi-aquatic lifestyle and ambush hunting mode are reflected in specific adaptations in the peripheral visual system. Design-based stereology and microspectrophotometry were used to assess spatial resolving power and spectral sensitivity of saltwater (*Crocodylus porosus*) and freshwater crocodiles (*Crocodylus johnstoni*). Both species possess a foveal streak that spans the naso-temporal axis and mediates high spatial acuity across the central visual field. The saltwater crocodile and freshwater crocodile have a peak spatial resolving power of 8.8 and 8.0 cycles deg^{-1}, respectively. Measurement of the outer segment dimensions and spectral absorbance revealed five distinct photoreceptor types consisting of three single cones, one twin cone and a rod. The three single cones (saltwater/freshwater crocodile) are violet (424/426 nm λ_{max}), green (502/510 nm λ_{max}) and red (546/554 nm λ_{max}) sensitive, indicating the potential for trichromatic colour vision. The visual pigments of both members of the twin cones have the same λ_{max} as the red-sensitive single cone and the rod has a λ_{max} at 503/510 nm (saltwater/freshwater). The λ_{max} values of all types of visual pigment occur at longer wavelengths in the freshwater crocodile compared with the saltwater crocodile. Given that there is a greater abundance of long wavelength light in freshwater compared with a saltwater environment, the photoreceptors would be more effective at detecting light in their respective habitats. This suggests that the visual systems of both species are adapted to the photic conditions of their respective ecological niche.

KEY WORDS: Microspectrophotometry, Retinal topography, Visual ecology, Chromophore shift, Reptile

INTRODUCTION

Crocodilians are apex predators that have dominated the water-edge niche for approximately 80 million years and, during this time, have become experts at ambushing prey while remaining concealed (Webb and Manolis, 1989; Nesbitt, 2011; Oaks, 2011). The *Crocodylus* genus has a wide distribution throughout the world's tropical regions. Species that occupy both river and coastal ocean habitats have a varied diet that includes insects, amphibians, fishes and small mammals (Lang, 1987). Crocodilians exhibit a diversity of social behaviours, including inflated posturing and snout lifting, which are used during courtship and mating to visually simulate increased strength and/or a dominant position (Garrick and Lang, 1977). The purpose and complexity of these behaviours vary from one species to another but the same visual cues are present across species found in different habitats, which suggests that vision is important in the crocodilian lifestyle. Although the general features of the crocodilian eye are known, there is little information available on the retinal specialisations of this taxon.

The crocodilian eye possesses a relatively large lens, a rod photoreceptor-dominated retina and a guanine-based tapetum lucidum, all features commonly associated with optimised sensitivity in dim light environments (Abelsdorff, 1898; Laurens and Detwiler, 1921). The eye is also equipped with a mobile slit pupil, which provides a high degree of control over the amount of light that reaches the retina during the day (Walls, 1942). Previous studies have described the retinal fine structure of the spectacled caiman, *Caiman crocodilus*, and the American alligator, *Alligator mississippiensis* (Tafani, 1883; Chievitz, 1889; Laurens and Detwiler, 1921), and measured the absorbance spectra of the visual pigments in *C. crocodilus*, *A. mississippiensis* and the Nile crocodile, *Crocodylus niloticus* (Dartnall and Lythgoe, 1965; Govardovskii et al., 1988; Sillman et al., 1991).

In this study, we have examined the only two species of crocodilian found in Australia: the world's largest living reptile, the saltwater crocodile, *Crocodylus porosus*, and the smaller freshwater crocodile, *Crocodylus johnstoni*. These two crocodiles occupy overlapping geographic habitats, where variations in salinity, competitive ability and nesting methods have created separate ecological niches (Webb et al., 1983; Tucker et al., 1997; Kay, 2005). *Crocodylus johnstoni* is endemic to Australia's northern regions, is commonly found further upstream, is less aggressive (Brien et al., 2013) and has a much narrower snout than *C. porosus* (A. Pearcy, Implications of skull shape for the ecology and conservation biology of crocodiles, PhD Thesis, Leiden University, 2011). Although both species are opportunistic feeders, *C. johnstoni* tends to eat smaller prey items and may hunt a higher proportion of fishes than *C. porosus* (Webb et al., 1983).

Crocodilians have demonstrated the ability to adapt to environmental conditions at a physiological level in their salt glands (Taplin et al., 1985); here we investigate whether this adaptability can be observed in the visual system. We examined aspects of retinal anatomy and physiology of *C. porosus* and *C. johnstoni* to identify adaptations for their specific visual-ecological niche. We assessed the topographic distribution of retinal ganglion cells and compared anatomical estimates of spatial resolving power (SRP). The spectral absorbance of the visual pigments expressed within the different retinal photoreceptor types was measured using microspectrophotometry.

SRP, or spatial acuity, is a measure of the ability to resolve spatial details in a visual scene. It is one of the fundamental characteristics

[1]School of Animal Biology, The University of Western Australia, Crawley, Western Australia 6009, Australia. [2]The Oceans Institute, The University of Western Australia, Crawley, Western Australia 6009, Australia. [3]Department of Biological Sciences, Macquarie University, North Ryde, New South Wales 2109, Australia.

*Author for correspondence (nicolas.nagloo@gmail.com)

Received 3 December 2015; Accepted 23 February 2016

Journal of Experimental Biology

Journal of Experimental Biology (2016) 219, 1394-1404 doi:10.1242/jeb.135673

of the visual system, which has been shown to be under intense selection pressure (Hughes, 1977). SRP depends on the posterior nodal distance of the eye and the minimum cell-to-cell spacing of retinal neurons (typically either photoreceptors or ganglion cells). In most species, retinal ganglion cells represent a bottleneck, where visual information converges before being sent to the visual centres of the brain and thus determining the upper limit of SRP. Detailed topographic information about retinal ganglion cell density provides insights into which areas of the visual field are attributed more neuronal resources and hence are potentially more relevant to the visual ecology of an animal.

The shape and position of retinal regions of high ganglion cell density have been correlated with the visual environment and lifestyle of many animal groups, including reptiles, birds and mammals (Hughes, 1977; Barbour et al., 2002; Coimbra et al., 2009). Both saltwater and freshwater crocodiles spend a significant proportion of their time waiting for the right time to ambush prey in a 'minimum exposure' posture with only the eyes and nostrils protruding above the water's surface. In this posture, the water surface makes up the majority of the bottom of the visual field and the visual horizon occurs along the riverbanks. This facilitates the detection of relevant visual cues along the water surface and along the riverbanks. According to the terrain theory (Hughes, 1977), this kind of open environment is best sampled by a band of high retinal ganglion cell density that mediates high detail discrimination ability over an extended area. We thus expect both species to possess a well-defined horizontal streak of high SRP along the visual horizon. The saltwater and freshwater crocodiles hunt prey of similar taxonomy and size (Webb et al., 1983) and adopt similar hunting and social behavioural strategies (Garrick and Lang, 1977). These similarities reduce the likelihood of a difference in selection pressures on the visual system from factors such as prey choice and conspecific interactions. Hence, the retinal specialisations of the saltwater and freshwater crocodiles are expected to be very similar despite approximately 12 million years of independent evolution between the two species (Webb and Manolis, 1989).

The spectral sensitivity of rod and cone photoreceptors and the number of different spectral types of cone photoreceptor influence both the absolute sensitivity of the visual system and the ability to extract chromatic information from the environment. The spectral sensitivity of photoreceptors can be tuned to optimise visual function by selective filtering of the incident light (Hart et al., 2000) or by changing the spectral absorbance characteristics of the visual pigments (through alterations to either the opsin protein or chromophore) located in the photoreceptor outer segments (Lythgoe, 1972; Bowmaker and Hunt, 2008). The spectral sensitivity of the photoreceptor complement of an animal is 'shaped' by both environmental and phylogenetic pressure. Because the majority of freshwater crocodiles live upstream in non-tidally affected freshwater rivers, the underwater light environment they experience will be relatively rich in long wavelength light compared with the more marine habitat inhabited by their saltwater counterparts (Lythgoe, 1972; Jerlov, 1976). Although saltwater crocodiles also spend some time in tidal rivers, which can have similar spectral properties to non-tidal rivers, they also venture out into the ocean, where shorter wavelength light is more abundant. If the predominant photic conditions in which both species of crocodile are found play an important enough role in their visual ecology, the visual pigments of freshwater crocodile photoreceptors would be predicted to have a higher photon catch than the saltwater crocodile photoreceptors in a stereotypical freshwater environment.

In this study, we investigated the topographic distribution of retinal ganglion cells and the spectral absorption characteristics of retinal photoreceptor visual pigments to determine whether differences in the ecological niches of each species are reflected in the visual system. Ecological adaptations of the visual system in both species are discussed.

MATERIALS AND METHODS

Animals

Two-year-old (juvenile) saltwater (*Crocodylus porosus* Schneider 1801) and freshwater (*Crocodylus johnstoni* Krefft 1873) crocodiles weighing 1.77±0.35 kg (mean±s.d.; n=15) and 1.68±0.79 kg (mean±s.d., n=4), respectively, were obtained from commercial breeders. Animals were kept in an indoor facility (12 h:12 h light: dark; temperature: 30°C) for up to 5 weeks and were euthanised using a lethal dose of sodium pentobarbital (150 mg kg^{-1}, intraperitoneal injection). All procedures were approved by The University of Western Australia Animal Ethics Committee (RA/3/100/1030).

Histological preparation of retinal whole-mounts

One eye was collected from each of three saltwater and two freshwater crocodiles for histological preparation of retinal whole-mounts to assess the topographic distribution of retinal ganglion cells. After euthanasia, the eye was immediately removed from the orbit and the axial length (AL) along the optic axis measured using a digital vernier calliper. The cornea was removed before the open eyecup was immersion fixed in 4% paraformaldehyde in 0.1 mol l^{-1} phosphate buffer (pH 7.2). After overnight fixation, retinae were dissected free of the retinal pigment epithelium and scleral eyecup. Radial cuts were made to allow the retina to be flattened. Retinae were whole-mounted on gelatinised slides and left overnight in chambers filled with formaldehyde vapours to dry (Coimbra et al., 2014). The retinal ganglion cell layer was then stained as described by Coimbra et al. (2006). Briefly, once adhered to the slide, retinae were rehydrated through a series of descending alcohol concentrations, stained with Cresyl Violet (0.1% in distilled water) and again dehydrated through a series of ascending alcohol concentrations before being cleared in xylene and coverslipped in Entellan New (Merck, USA).

Histological criteria for the differentiation of retinal ganglion cells

Nissl-stained ganglion cells were differentiated from displaced amacrine cells and glial cells situated within the ganglion cell layer by their staining characteristics, size and shape. Displaced amacrine cells were consistently smaller than ganglion cells and had a more uniform and paler staining profile. Glial cells had an irregular shape and stained very darkly (Fig. 1). The soma of retinal ganglion cells were the largest and revealed a granular cytoplasm with a frequently visible nucleus. Displaced retinal ganglion cells (within the inner nuclear layer) were not counted.

Stereological sampling and estimation of retinal ganglion cell number

The outline of the retina was digitised using a ×4 NA 0.17 objective lens and a motorised stage (MAC200; Ludl Electronics Products, USA) attached to a computer running Stereo Investigator software (MBF Bioscience, USA). The optical fractionator probe (West et al., 1991) modified for the retina (Coimbra et al., 2009) was used to sample the retinal ganglion cell layer with a ×60 NA 1.35 oil immersion lens. Briefly, a counting grid was superimposed on the

Journal of Experimental Biology (2016) 219, 1394-1404 doi:10.1242/jeb.135673

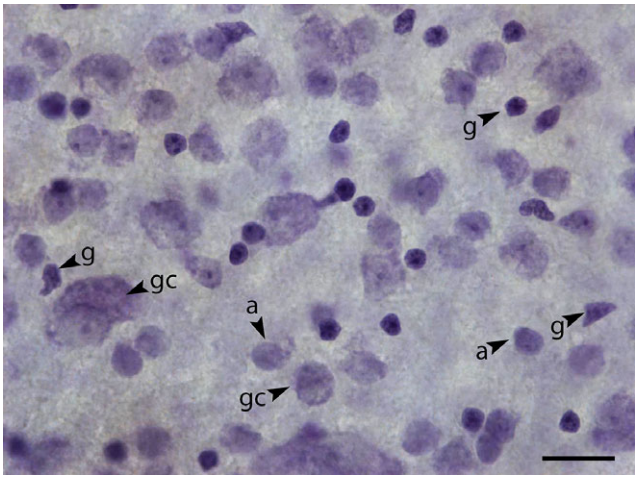

Fig. 1. Nissl-stained cells in the dorsal region of the crocodile retina (*Crocodylus johnstoni*). a, Displaced amacrine cells; g, glial cells; gc, retinal ganglion cells. Scale bar, 20 µm.

digitised outline of the retina, giving a sampling location for each grid point within the outline. Each sampling location represented the area of one square of the grid but only a fraction of that area was sampled, using a sampling frame of set size at each location (Table 1). All retinal ganglion cells within the area of the sampling frame were counted by focusing through the retinal ganglion cell layer. Each count was used to estimate the number of retinal ganglion cells for each grid location (Coimbra et al., 2009):

$$N = \Sigma Q \times 1/a_{\mathrm{sf}}, \quad (1)$$

where ΣQ is the sum of the retinal ganglion cells counted in each sampling location, a_{sf} is the ratio of the sampling frame area to the counting grid area used in this sampling regime and N is an estimate of the retinal ganglion cell number in the area represented by the sampling frame. The sum of all retinal ganglion cell estimates from all sampling locations provides an estimate of the total number of retinal ganglion cells. Cell densities at each sampling location were expressed as standardised densities in cells mm^{-2} (Coimbra et al., 2014; Garza-Gisholt et al., 2014).

Initial counts revealed a region of high cell density surrounding a furrowed line across the retina spanning the naso-temporal axis. This high density region, referred to hereafter as the foveal region, was resampled at double the resolution using a secondary sampling protocol (Coimbra et al., 2013) to more efficiently assess the rapid changes in cell density within this region (Table 1).

Mapping of retinal ganglion cells

R software (R Development Core Team, 2015) was used for all mapping and interpolation. A thin plate spline was used to interpolate cell density (cells mm^{-2}) data between sampling locations and establish a series of iso-density lines, which were used to construct a topographic map of the retina (Hemmi and Grünert, 1999; Garza-Gisholt et al., 2014). The thin-plate spline is a geometric function that allows simultaneous interpolation and smoothing of the data. The extent of smoothing can be controlled by two parameters. The first is the power of the polynomial used to fit the function to the sampling location values, and the second is the lambda value, which changes the roughness penalty of the function (Garza-Gisholt et al., 2014). In this case, the 'tps' function from the 'fields' package was used for the thin plate spline (Nychka et al., 2015) with a second-order polynomial fitting and the lambda value determined by general cross-validation.

Spatial resolving power

The SRP was calculated according to the Nyquist sampling theorem (Williams and Coletta, 1987) using anatomical measures. The Nyquist sampling theorem states that a signal can be sampled and reconstructed without aliasing if the highest signal frequency does not exceed $1/2s$, where s is the distance between receptors (samples). This places a limit on the SRP that can be obtained from a given sampling array of retinal ganglion cells, and is known as the Nyquist limit of the sampling array (Williams and Coletta, 1987). The two eye measures used for calculating the spatial resolving power of the eye from anatomy were the PND and the peak retinal ganglion cell density. Because it was not possible to

Table 1. Sampling parameters and total number of retinal ganglion cells in the two species of Australian crocodile

Specimen	Counting grid (µm)	Sampling frame (µm)	Area (mm^2)	No. sites	No. retinal ganglion cells	CE[a]
Crocodylus porosus						
Cpo1R						
Periphery	1500×1500	150×150	383	149	459,393	0.065
Streak	750×750	75×75	74	124	468,478	0.034
Total	–	–	457	273	928,871	
Cpo2L						
Periphery	1500×1500	150×150	368	141	495,400	0.061
Streak	750×750	75×75	65	119	424,500	0.033
Total	–		433	260	919,900	
Cpo3L						
Periphery	1500×1500	150×150	385	143	489,900	0.045
Streak	750×750	75×75	84	138	535,210	0.025
Total	–	–	469	281	1,025,110	
Crocodylus johnstoni						
Cjo1L						
Periphery	1500×1500	150×150	318	109	398,600	0.056
Streak	750×750	75×75	79	128	486,627	0.043
Total	–	–	397	237	885,227	
Cjo2L						
Periphery	1500×1500	150×150	299	121	559,000	0.069
Streak	750×750	75×75	36	56	302,080	0.031
Total	–	–	335	177	861,080	

[a]Schaeffer coefficient of error associated with each sampling protocol for all retinae (Glaser and Wilson, 1998; Slomianka and West, 2005).

Journal of Experimental Biology (2016) 219, 1394-1404 doi:10.1242/jeb.135673

directly measure the PND, it was estimated by multiplying the measured AL by 0.57, the ratio between axial and posterior nodal distance (PND), which has previously been defined for cathemeral and crepuscular animals by Pettigrew et al. (1988). These measures were used to calculate image magnification in the eye (retinal magnification factor, RMF; Pettigrew et al., 1988):

$$\mathrm{RMF} = 2\pi\mathrm{PND}/360 \quad (2)$$

and SRP (Snyder and Miller, 1977):

$$f_N = 0.5 \times \mathrm{RMF} \times \left(\frac{2D}{\sqrt{3}}\right)^{1/2}, \quad (3)$$

where f_N is the Nyquist limit in cycles per degree and D is the peak cell density.

A hexagonal lattice array was assumed as that would give the minimal cell-to-cell distance and therefore the maximum SRP with a given PND (Williams and Coletta, 1987). The maximum SRP value assumes that all retinal ganglion cells sampled are involved in detail discrimination and that photoreceptor density and distribution is such that photoreceptor density is always higher than retinal ganglion cell numbers in any given area.

Microspectrophotometry of photoreceptor outer segments

To measure the spectral absorbance characteristics of the visual pigments contained in the different retinal photoreceptor types in both species, we collected six eyes from four saltwater crocodiles and one eye each from two freshwater crocodiles. Eyes were dissected under infrared light to minimise bleaching of the visual pigments as described in Hart (2004). Small pieces of retinal tissue were mounted between glass coverslips in a drop of 8% dextran in 0.1 mol l^{-1} phosphate buffered saline (pH 7.2) and mounted on the stage of a single-beam wavelength-scanning microspectrophotometer (Hart, 2004). Photoreceptors were viewed indirectly under infrared illumination using an image converter (Electroviewer 7215, Electrophysics, USA). Visual pigment absorbance spectra (330–800 nm, 1 nm intervals) were made by scanning first the outer segment of the photoreceptor (sample scan) and then a tissue-free area adjacent to the photoreceptor (baseline scan) (Hart, 2004). Photoreceptors were then bleached with full-spectrum white light, and post-bleach measurements (sample and baseline scans) were made to confirm that the pigment in the outer segment was photolabile. The length and width of all outer segments was measured using a calibrated acetate sheet overlayed on the monitor (Hart, 2004; Hart et al., 2011). Spectra that satisfied criteria described elsewhere (Levine and MacNichol, 1985; Hart et al., 1998, 1999) were kept for further analysis.

Analysis of absorbance spectra

Raw absorbance data were smoothed using an unweighted running average before estimating the peak (maximum) and long wavelength offset (mean absorbance from 680 to 780 nm) absorbance values. These values were then used to normalise the data. A regression line was then fitted to absorbance values between 30% and 70% of the peak on the long wavelength side of the curve to predict the wavelength of maximum absorbance (predicted λ_{max}). This region of the curve is used as it is the least likely to be distorted by photostable pigments and scattering artefacts (MacNichol, 1986). The predicted λ_{max} was then used to seed the Govardovskii equations for A_1 or A_2 visual pigment absorbance templates and the resulting template was overlayed on the smoothed data. The number of points used in the initial smoothing of the data was then iteratively adjusted to minimise deviation of the normalised absorbance data from the template data over the range of wavelengths corresponding to 80% normalised absorbance on the short wavelength limb to 20% normalised absorbance on the long wavelength limb.

In an attempt to explain the remaining deviations between the normalised absorbance curve of a photoreceptor and the pure A_1/A_2 visual pigment template, a mixed chromophore model was used (Temple et al., 2010; de Busserolles et al., 2015). The model assumed that each photoreceptor contained only one opsin, but possibly a varying percentage of A_1- and A_2-based chromophores. The percentage of A_1 to A_2 chromophores was estimated with a least squares procedure by fitting the normalised absorbance data to the model curve. The relationship between A_1 and A_2 λ_{max} values was obtained from Parry and Bowmaker (2000).

To further assess whether opsin and/or chromophore changes were responsible for observed differences in the spectral sensitivity of photoreceptors between species, the relationship between the λ_{max} values of the smoothed absorbance curves and the bandwidth of the absorbance curves at 50% of the peak (hereafter referred to as bandwidth) were compared with the relationship of pure A_1/A_2 visual pigment templates across a range of λ_{max} values.

Ocular media transmittance measurements

The effective spectral sensitivity of a photoreceptor is also determined by the spectral transmittance characteristics of the ocular media, primarily the cornea and lens. Therefore, five eyes from four saltwater crocodiles and both eyes of one freshwater crocodile were used for spectral transmission measurements of the cornea and lens with a spectroradiometer (USB4000; Ocean Optics, USA). Light from a xenon lamp (PX-2, Ocean Optics) was delivered through a 100 µm diameter SMA-terminated optical fibre (Ocean Optics), collimated by a lens (74-UV; Ocean Optics) and projected onto isolated specimen lenses and corneas mounted in air. Transmitted light was collected on the other side of either the lens or the cornea with a 1000 µm SMA-terminated optical fibre (Ocean Optics) and matching collimating lens as described by Hart et al. (2012). At least three measurements were made per eye and normalised to the average transmittance between 700 and 800 nm, where the transmittance was stable and at the maximum. The normalised transmittance was then averaged at the eye and individual level to obtain the average transmittance for both the cornea and the lens. The combined transmittance of cornea and lens was obtained by multiplying the average normalised curve for both types of ocular media.

Effective spectral sensitivity

For both species of crocodile, the effective quantal spectral sensitivity function for each cone photoreceptor type was estimated as the product of the calculated spectral absorptance of the outer segment and the spectral transmittance of the combined ocular media. Outer segment absorptance was calculated using a specific (decadic) absorbance of 0.0153 μm^{-1} and the mean length for spectrally identified outer segments measured during the microspectrophotometric procedures (Warrant and Nilsson, 1998). Visual pigment absorbance spectrum templates (Govardovskii et al., 2000) of the appropriate λ_{max} (or template mixtures from the mixed-chromophore model where more than one chromophore was assumed to be present) were used rather than measured absorbance spectra.

RESULTS

The gross morphology of the eye of Australian crocodiles confirms previous descriptions of the crocodilian eye in other species

Journal of Experimental Biology (2016) 219, 1394-1404 doi:10.1242/jeb.135673

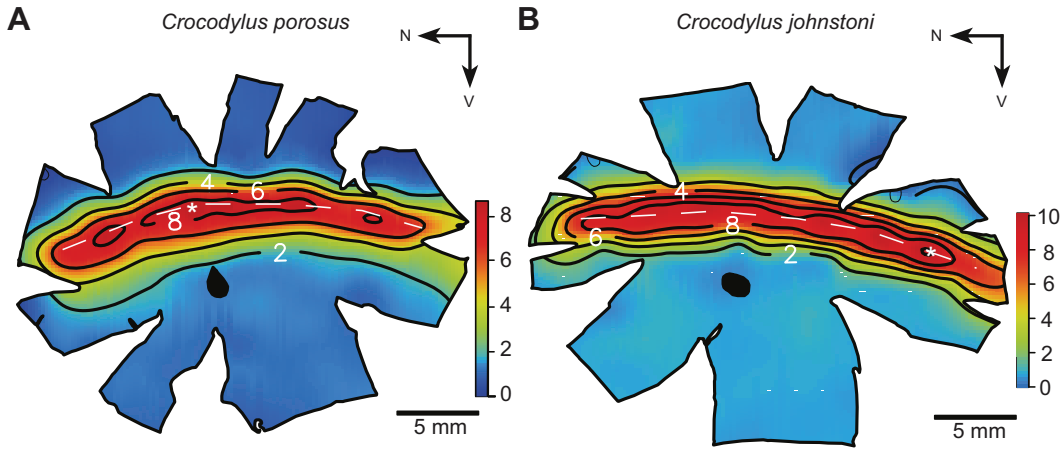

Fig. 2. Topography of retinal ganglion cells in two species of Australian crocodiles. (A) The saltwater crocodile, *Crocodylus porosus*. (B) The freshwater crocodile, *Crocodylus johnstoni*. Iso-density lines are plotted at intervals of 2000 cells mm^{-2}. All numbers (and colour scale) indicate ×1000 cells mm^{-2} and both retinae are from left eyes. N, nasal; V, ventral. White dashed lines indicate the furrow visible by the naked eye, providing the approximate position and extent of the foveal slit, and white asterisks indicate the location of peak cell density in this representative retina. Note: location of peak cell densities varies between individuals but stays within the streak, suggesting that there is no one peak region within the streak in either species.

(Laurens and Detwiler, 1921). Both Australian species possess a bright yellow iris, a slit pupil and a relatively large lens. The similarity in age and mass of all juvenile saltwater and freshwater crocodiles used in this study is reflected in the similarity in the PNDs (estimated mean±s.d. PND of 8.9±0.2 and 8.0±0.0 mm for *C. porosus* and *C. johnstoni*, respectively) and retinal areas (mean±s.d., 453±18 and 366±44 mm^2 for the two species, respectively). After removing the cornea and lens, a furrowed line in the retina, dorsal to the optic disk and extending across the naso-temporal axis, could be easily observed by the naked eye in all retinae (Fig. 2). A tapetum lucidum is present in both species and has the highest reflectance behind the furrowed foveal slit.

The topography of retinal ganglion cells and spatial resolving power

Stereological measurements of retinal ganglion cell distribution revealed similar topographies for both species (Fig. 2). Estimates of total retinal ganglion cell numbers were very close (mean±s.d. 958,000±58,000 and 873,000±17,000 for *C. porosus* and *C. johnstoni*, respectively, with values rounded to the nearest thousand cells; Table 1) and both species showed a high density band of retinal ganglion cells extending across the retina, slightly dorsal of the optic nerve head. At the centre of this well-defined horizontal streak sits the shallow furrow or superficial horizontal fovea described above (Fig. 2). The peripheral region of the retina is fairly homogeneous, with approximately 2000 cells mm^{-2} distributed over most of the non-specialised retinal area in both species. Approximately 48% of the total number of retinal ganglion cells is found within the region sampled at higher resolution, which constitutes 16% of the total retinal area. The average ganglion cell density at the centre along the streak is approximately four times that of the peripheral regions. The mean±s.d. peak retinal ganglion cell density was 11,083±448 and 11,375±756 cells mm^{-2} in *C. porosus* and *C. johnstoni*, respectively (Table 2).

Based on the PND and the peak retinal ganglion cell density, the SRP was estimated to be 10% higher in *C. porosus* (8.8±0.4 cycles deg^{-1}) compared with *C. johnstoni* (8.0±0.3 cycles deg^{-1}; see Table 2 and Materials and methods for details).

Morphological and spectral characterisation of photoreceptor types

Based on morphological observations and recorded absorbance spectra, five different photoreceptor spectral types were identified in both species of crocodile. Three types of single cones, one type of twin cone and one type of rod were present in both species. Two of the single cone types were similar in size and morphology (mean outer segment width of 1.0–1.5 µm and length of 10.0–12.0 µm) but contained either a medium wavelength sensitive (MWS) or a long wavelength sensitive (LWS) visual pigment. The third single cone type was smaller (mean outer segment width of 1.7–1.9 µm and length of 7.4–8.0 µm) and contained a short wavelength sensitive

Table 2. Spatial resolving power for *Croodylus porosus* and *C. johnstoni* estimated from posterior nodal distance and peak retinal ganglion cell density while assuming a hexagonal lattice

Species	Eye ID	Axial length (mm)	PND (mm)	Peak (cells mm^{-2})	Peak (cells mm^{-1})	RMF	Hexagonal lattice SRP
C. porosus	cpo01re	15.9	9.0	11,560	108	0.2	9.1
	cpo02le	15.9	9.0	11,020	105	0.2	8.9
	cpo3le	15.1	8.6	10,670	103	0.2	8.3
	Mean	15.6	8.9	11,083	105	0.2	8.8
	s.d.	0.4	0.2	448.4	2.1	0.0	0.40
C. johnstoni	cjo02le	14.0	8.0	10,840	104	0.1	7.8
	cjo03le	14.0	8.0	11,910	109	0.1	8.2
	Mean	14.0	8.0	11,375	107	0.1	8.0
	s.d.	0.0	0.0	756.6	3.5	0.0	0.27

PND, posterior nodal distance; RMF, retinal magnification factor; SRP, spatial resolving power.

Journal of Experimental Biology

Journal of Experimental Biology (2016) 219, 1394-1404 doi:10.1242/jeb.135673

Table 3. Morphological characterisation of photoreceptor types in *Crocodylus porosus* and *C. johnstoni*

Species	Photoreceptor type	No. cells measured	Mean OS length (µm)	Mean OS width (µm)
C. porosus	Rods	20	28.9±4.96	5.0±0.60
	SWS single	4	8.0±1.41	1.9±0.85
	MWS single	8	11.0±3.07	1.1±0.42
	LWS single	11	11.2±4.15	1.0±0.15
	LWS twin	28	10.5±1.55	1.2±0.36
C. johnstoni	Rods	8	19.9±4.64	4.7±0.65
	SWS single	13	7.4±1.80	1.7±0.83
	MWS single	7	12.0±3.56	1.5±0.58
	LWS single	17	10.2±2.74	1.5±0.45
	LWS twin	22	9.8±2.20	1.5±0.45

LWS, long wavelength sensitive; MWS, medium wavelength sensitive; OS, outer segment; SWS, short wavelength sensitive. Means are presented ±s.d.

Table 4. Spectral sensitivity of photoreceptor types in *Crocodylus porosus* and *C. johnstoni* measured using microspectrophotometry

Species	Photoreceptor type	No. cells measured	Mean smoothed λ_{max} (nm)	Mean A_1 %
C. porosus	Rods	75	502.9±2.6	96.9±7.5
	SWS single	3	424.3±4.5	33.6±15.8
	MWS single	11	502.4±5.3	80.4±32.9
	LWS single	25	546.2±4.6	96.5±13.5
	LWS twin	19	546.4±3.6	98.5±4.5
C. johnstoni	Rods	50	509.9±2.6	45.6±18.7
	SWS single	14	426±4.5	32.9±21.58
	MWS single	7	510.4±5.7	38.8±25.3
	LWS single	23	554.1±5.3	72.6±17.3
	LWS twin	25	555.2±6.0	68.7±16.6

LWS, long wavelength sensitive; MWS, medium wavelength sensitive; SWS, short wavelength sensitive. Means are presented ±s.d.

(SWS) visual pigment (Table 3). The twin cones were always found in pairs of outer segments attached to a fused pair of inner segments, but the two members were otherwise identical in size to the LWS single cones and both contained the LWS visual pigment. The rod photoreceptor was the most distinct, with an outer segment 4.7–5.0 µm wide and 20.0–29.0 µm long (Table 3). None of the photoreceptor types possessed oil droplets.

Microspectrophotometry was used to measure the absorbance spectra of visual pigments contained in the five different photoreceptor types of *C. porosus* and *C. johnstoni*. The spectral location of the peak value of the smoothed absorbance data was used to estimate the λ_{max} of the outer segment and provide a stable comparison across species (Fig. 3). In *C. porosus*, the cones had mean±s.d. λ_{max} values at 424.3±4.5 nm (SWS), 502.4±5.3 nm (MWS single cones), 546.2±4.6 nm (LWS single cones) and 546.4±3.6 nm (LWS twin cones). Rods were the most abundant photoreceptor encountered and had a mean±s.d. λ_{max} of 502.9±2.6 nm. *Crocodylus johnstoni* had a similar complement of photoreceptors, but λ_{max} values were shifted towards longer wavelengths for all photoreceptor types except the SWS single cone (424±4.5 nm). The remainder of the cones in *C. porosus* had λ_{max} values at of 510.4±5.7 nm (MWS single cones), 554.1±5.3 nm (LWS single cones) and 555.2±6.0 nm (LWS twin cones). The rod photoreceptor had a λ_{max} at 509.9±2.6 nm (Table 4).

A mixed chromophore model was used to estimate the proportion of A_1- versus A_2-chromophore-based visual pigments within a given photoreceptor type. Excluding the SWS single cones, the model predicted a mean A_1-chromophore content across all photoreceptor types of 93.1±8.5% and 60.0±18.5% for *C. porosus* and *C. johnstoni*, respectively. The SWS single cone of both species has a very similar peak absorbance and the model predicted a similar proportion of A_1 visual pigment, with 33.6±15.8% for *C. porosus* and 32.9±21.6% for *C. johnstoni*. Microspectrophotometric data of visual pigments are less reliable at short wavelengths because of increased measurement (instrumental) noise and increased scattering and absorption by biological and optical structures, and there is also a relatively smaller shift in λ_{max} and bandwidth when the chromophore is substituted for visual pigments with shorter λ_{max} values. Consequently, the fits of the mixed chromophore model to

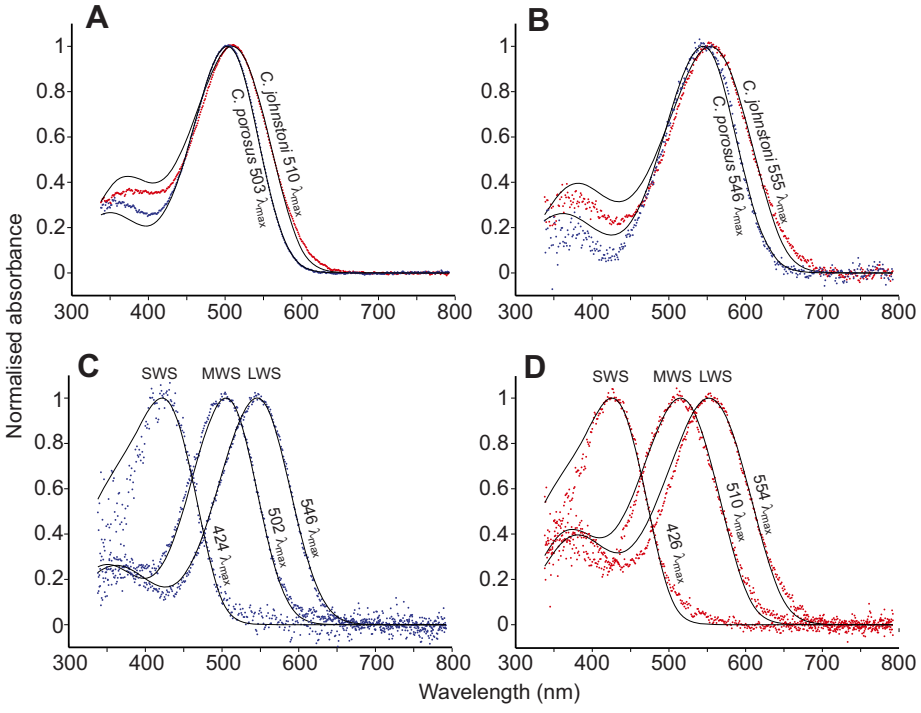

Fig. 3. Normalised absorbance of averaged spectra for *Crocodylus porosus* and *C. johnstoni* with A_1 and A_2 templates overlayed on measurements, respectively. (A) Rods. (B) Twin cones. (C,D) Single cones for saltwater (C, blue dots) and freshwater crocodiles (D, red dots). Mean smoothed λ_{max} for each pigment is listed next to the spectral sensitivity curve.

Journal of Experimental Biology (2016) 219, 1394-1404 doi:10.1242/jeb.135673

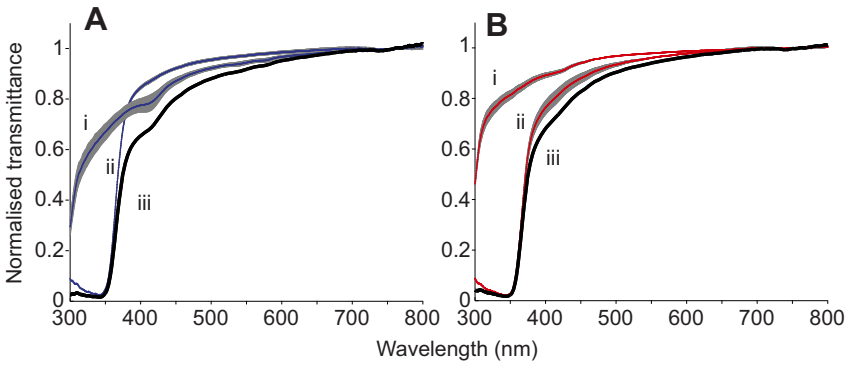

Fig. 4. Normalised spectral transmittance (mean± s.e.m.) of the ocular media in the two species of Australian crocodile. Data are for (A) *Crocodylus porosus* and (B) *C. johnstoni* for the (i) cornea, (ii) lens and (iii) combined transmittance, between 300 and 800 nm. Standard error is indicated by the grey shading; blue and red lines represent transmittance curves of *C. porosus* and *C. johnstoni*, respectively, for the cornea and lens individually; black lines represent combined curves (the 50% transmittance cut-off for the combined curve occurs at 374 and 375 nm for *C. porosus* and *C. johnstoni*, respectively).

the SWS pigment data may be less reliable than for the other photoreceptor types.

Spectral transmittance of the ocular media

In an attempt to identify other mechanisms that may affect the spectral sensitivity in the two species, we measured the spectral transmittance of the cornea and lens (Fig. 4). The wavelength of 0.5 normalised transmittance of the combined ocular media of *C. porosus* and *C. johnstoni* was 374 and 375 nm, respectively. Transmittance at short wavelengths is largely determined by the spectral characteristics of the lens, which absorbs considerably more light than the cornea below 350 nm.

The spectral filtering effects of the ocular media at shorter wavelengths results in a spectral shift of approximately 10 nm in the peak sensitivity of the SWS photoreceptor towards longer wavelengths in both species (Fig. 5). The spectral properties of the lens and cornea may also block ultraviolet light that would otherwise stimulate the β-peak of the visual pigments.

DISCUSSION

We investigated the SRP and spectral sensitivity of *C. porosus* and *C. johnstoni* to identify visual adaptations that may reflect the visual ecology of each crocodile species. An analysis of the spatial distribution of retinal ganglion cells indicates that both species possess a similar topographic arrangement of retinal ganglion cells and a similar SRP. In contrast, the spectral sensitivities of photoreceptors in both species differ, with freshwater crocodiles having longer wavelength λ_{max} across all photoreceptor classes.

Spatial resolving power

Two main factors affect maximal SRP: eye size and peak retinal ganglion cell density. The difference in mean peak retinal ganglion cell density between juvenile saltwater and freshwater crocodiles (200 cells mm^{-2}) is slight and well within the measurement error. This suggests that the difference in SRP (1 cycle deg^{-1}) between species is predominantly a result of the difference in AL of the eyes of juvenile saltwater and freshwater crocodiles. Considering that eye size has been demonstrated to increase with body size for mammals (<30 kg body mass) and birds, the difference in mean (±s.d.) mass of our juvenile saltwater and freshwater crocodiles (1.77±0.35 and 1.68±0.79 kg, respectively) may explain differences in AL and therefore SRP (Kiltie, 2000). Growth rate and body size in crocodilians is known to vary considerably with environmental conditions, feeding rate and, ultimately, food conversion rates (Webb and Manolis, 1989; Webb et al., 1991; Tucker et al., 2007). This suggests that eye size and therefore SRP vary more within species than between species. If eye size remains dependent on body size until both species stop growing and retinal ganglion cell density remains constant, it is likely that there will be a greater difference in SRP as the average maximum size for saltwater and freshwater crocodiles differs greatly (approximately 500 kg, 5.2 m total length and approximately 25 kg, 2.0 m total length, respectively). Although the crocodiles in this study are still juveniles (AL=15 mm), their SRP is relatively low compared with animals such as diurnal geckoes and the Carolina anole, *Anolis carolinensis* (SRP=13.2 and 16.9 cycles deg^{-1}, respectively), which possess much smaller eye and body size (AL=4.5 and 5.0 mm, respectively) (Makaretz and Levine, 1980; Röll, 2001; Hall, 2008). In contrast, nocturnal geckoes possess a much lower SRP of 3.2 cycles deg^{-1} than diurnal geckoes, while possessing eye and body sizes (AL=4.5 mm) similar to those of diurnal geckoes (Makaretz and Levine, 1980; Röll, 2001; Hall, 2008). The ratio of SRP to AL of our juvenile crocodiles (0.6) is closer to nocturnal geckoes (0.7) than diurnal geckoes (3.0) and *A. carolinensis* (3.4). Combining this

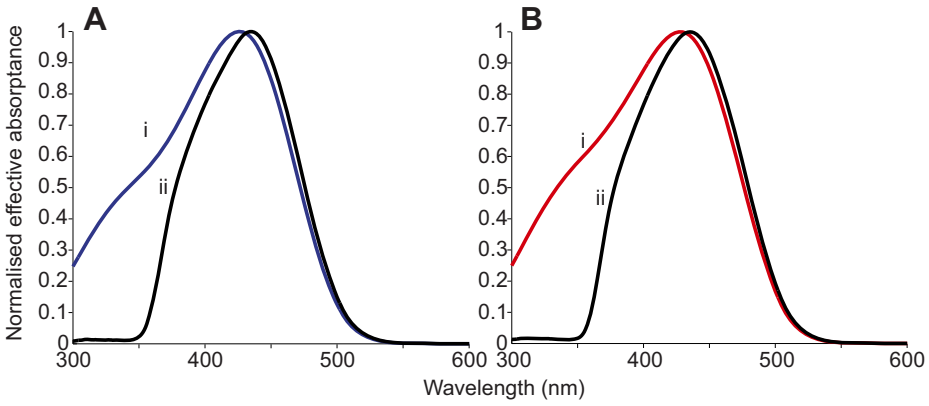

Fig. 5. Normalised effective absorptance spectra of short wavelength sensitive (SWS) pigments in the two species of Australian crocodile. (A) *Crocodylus porosus*. (B) *Crocodylus johnstoni*. (i) Outer segment absorptance based on the spectral absorbance curve produced by the mixed chromophore model for SWS pigments (blue for *C. porosus* and red for *C. johnstoni*). (ii) Absorptance curve corrected for transmittance of the combined ocular media (black for both species).

Journal of Experimental Biology (2016) 219, 1394-1404 doi:10.1242/jeb.135673

with the non-diurnal lifestyle of crocodiles suggests that their visual system may prioritise other aspects of visual performance such as light sensitivity over visual acuity, as observed in many nocturnal animals.

Specialised distribution of retinal ganglion cells and its relevance

Crocodylus porosus and *C. johnstoni* possess a horizontal foveal slit that spans the naso-temporal axis in the middle of a streak across the equator of the retina. Both species also have similar total numbers of retinal ganglion cells and similar peak cell densities. Similar structures are described in *A. mississippiensis* (Laurens and Detwiler, 1921), suggesting a common retinal organisation across crocodilians.

The elongated shape of the streak allows it to mediate enhanced SRP over an extended area of the visual field. This facilitates surveying of the surroundings for visual cues while reducing the need for head movements when eye movement has reached its limits. Because crocodilians are unable to focus underwater (Fleishman et al., 1988), tasks that require higher SRP are likely to occur above the water level. Crocodiles are well known for using a 'minimum exposure' position (Webb and Manolis, 1989), where only the eyes and nostrils are above the water level when tracking prey items. Adopting this position aligns the image of the riverbank with the retinal streak and enables them to survey potential prey items with enhanced fine detail discrimination while remaining concealed. This can also facilitate the detection of the eyes of competing crocodiles protruding above the water surface. Bigger crocodiles are territorial and can be quite aggressive (especially the saltwater crocodile), making their early detection crucial for the survival of juvenile (or younger) crocodiles (Webb and Manolis, 1989). In addition, the brightest region of the tapetum lucidum is located behind the streak, providing enhanced reflection of light in this retinal region. This would increase the sensitivity of the streak when operating at low light levels (Abelsdorff, 1898; Garten, 1907).

The very narrow and superficial fovea in the vertical centre of the streak implies less lateral displacement of retinal ganglion cells than what occurs in the fovea of diurnal lizards (Chievitz, 1889; Laurens and Detwiler, 1921; Röll, 2001; Barbour et al., 2002). Given the fact that diurnal geckoes are foveated while nocturnal geckoes are not, the superficial fovea of crocodilians may represent a halfway point between the two that reflects their arrhythmic lifestyle (Röll, 2001; Barbour et al., 2002). Alternatively, the similar ratio of eye size and SRP described above for crocodile juveniles and nocturnal geckoes may suggest that the crocodilian fovea is vestigial. If the fovea is still functionally relevant, the elongated shape would provide higher SRP in zones of the visual field where essential visual cues occur.

The ambush hunting strategy most common in crocodilians is well supported by the retinal specialisations in Australian crocodiles revealed by this study. This creates a set of complementary

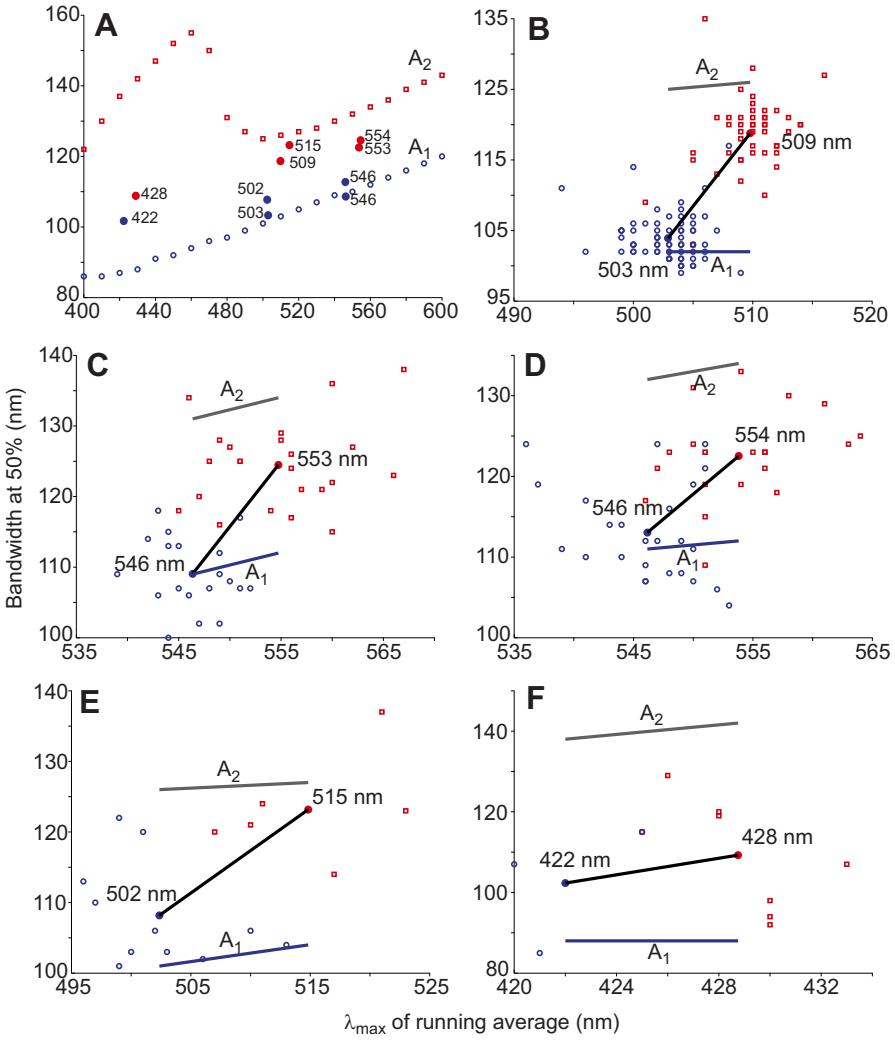

Fig. 6. Change of full-width at half maximum (50%) bandwidth with the λ_{max} of pure A_1/A_2 visual pigments compared with crocodile photoreceptors. (A) Bandwidth and λ_{max} of A_1 and A_2 visual pigment templates across a range of wavelengths. (B) Rods. (C) Long wavelength sensitive (LWS) twin cones. (D) LWS single cones. (E) Medium wavelength sensitive single cones. (F) Short wavelength sensitive single cone. Filled circles are mean bandwidth and mean λ_{max} values of photoreceptor types in *Crocodylus porosus* (blue) and *C. johnstoni* (red). Individual measurements are represented in open blue circles for *C. porosus* and open red squares for *C. johnstoni*. The top line labelled A_2 and bottom line labelled A_1 display the bandwidth for their respective templates across the same λ_{max} values as the mean for each photoreceptor.

Journal of Experimental Biology (2016) 219, 1394-1404 doi:10.1242/jeb.135673

adaptations that can greatly reduce the chance of being detected by prey while increasing hunting success in their given ecological niches.

Spectral sensitivity of retinal photoreceptors

Based on photoreceptor size and spectral sensitivity, it is possible to identify five different photoreceptor types present in *C. porosus* and *C. johnstoni*: SWS, MWS and LWS single cones, LWS twin cones and a MWS rod. This complement of photoreceptors differs slightly from that of the other crocodilians studied to date. The photoreceptors of the American alligator absorb maximally at 443 nm (single cone), 535 nm (single cone), 566 nm (double cone principal member), 503 nm (double cone accessory member) and 503 nm (rod) (Sillman et al., 1991). The photoreceptor complement of the spectacled caiman, in contrast, seems to have a reduced spectral range with maximal absorbances at 430 nm (single cone), 535 nm (single cone), 535 nm (double cone principal member), 535 or 506 nm (double cone accessory member) and 506 nm (rod) (Govardovskii et al., 1988). The only other information on crocodilian visual pigments is the two extracted pigments of the Nile crocodile with maximal absorbance at 507 and 527 nm mentioned in Dartnall and Lythgoe (1965).

In contrast to the American alligator and spectacled caiman, both the saltwater and freshwater crocodiles possess an extra single cone (LWS cone) with a λ_{max} value of 546 and 554 nm, respectively. Although the Australian crocodile species have a greater number of single cone types, they have fewer spectrally distinct cone types than the American alligator because the members of the double cone in the American alligator can have two different λ_{max} values (Sillman et al., 1991). Although double cones have been demonstrated to be used in colour vision in one species of reef fish, *Rhinecanthus aculeatus* (Pignatelli et al., 2010), in animals more closely related to crocodiles, such as birds and turtles, they are thought to be used to gather information for achromatic pathways (Richter and Simon, 1974; Maier and Bowmaker, 1993; Vorobyev et al., 1998). Depending on the function of the double cones, this may mean that the American alligator has the potential for either dichromatic or tetrachromatic colour vision, while Australian crocodiles have the potential for trichromacy. A higher number of spectrally distinct cones would provide better colour constancy while a broader spectral range would increase the probability of catching photons.

In the freshwater crocodile, the λ_{max} of all photoreceptor types, except for the SWS single cones, were shifted towards longer wavelengths. Because the saltwater crocodile has a higher percentage of A_1 visual pigment in its photoreceptors (93.1±8.5% and 60.0±18.5%, excluding the SWS single cone), this suggests that a changing mixture of A_1 and A_2 visual pigments within the photoreceptor types might be responsible for the spectral sensitivity shift. A complete or partial shift from A_1- to A_2-chromophore-based visual pigments from a marine to freshwater habitat has been well documented in species such as marine and freshwater turtles and several teleosts that change habitat (Liebman and Granda, 1971; Lythgoe, 1972; Loew and Govardovskii, 2001). Switching to an A_2 visual pigment shifts the peak sensitivity of an A_1 visual pigment to longer wavelengths but also broadens the absorbance curve of the pigment (Whitmore and Bowmaker, 1989; Hárosi, 1994; Parry and Bowmaker, 2000). This increases the chance of photon capture in many freshwater habitats where the dissolved organic matter selectively absorbs short wavelength light and reduces the overall number of photons available (Jerlov, 1976; Kirk, 1980). The change in the bandwidth of the absorbance curves of the photoreceptors from the saltwater crocodile to the freshwater crocodile reflect the changes that one would expect when changing from an A_1 to an A_2 pigment (Fig. 6). However, the American alligator, the spectacled caiman and the Nile crocodile all possess only A_1 visual pigments (Dartnall and Lythgoe, 1965; Govardovskii et al., 1988; Sillman et al., 1991) even though they live in freshwater areas such as the Nile river and the Everglades, which are rich in dissolved organic matter and particulates (Chen et al., 2010; El-Magd et al., 2014). This suggests that different photic conditions may not be the only driver for A_1–A_2 differences observed in saltwater and freshwater crocodiles. The only photoreceptor that remains relatively unchanged between the two species appears to be the SWS single cone, although further data are required to establish whether this reflects photoreceptor-type-specific variation in A_1:A_2 ratios across species.

Alternative reasons for an A_1–A_2 shift in visual pigments has been examined in several species such as salamanders, bullfrogs, carp, salmonids and the Japanese dace (Ala-Laurila et al., 2004, 2007; Ueno et al., 2005; Temple et al., 2006). These studies revealed a correlation between day length, temperature and migration to different photic conditions as driving factors for shifting from an A_1 to an A_2 pigment, while acknowledging that other external factors may be present. Annual variation in the water levels of rivers and lakes in the Northern Territory (Australia) result in shallower, warmer and less turbid rivers in summer and a higher turbulence and slightly cooler rivers in winter (Erskine et al., 2003). These variations in river conditions give rise to water temperature changes not unlike the mean annualised sea surface temperature range of 26–30°C. This, combined with the geographical proximity of *C. johnstoni* to *C. porosus* (Tucker et al., 1997; Kay, 2005), suggests the lack of a significant difference in temperature or day length to account for the difference in chromophore content.

In an attempt to identify other mechanisms that may produce differences in the effective absorbance of photoreceptors in these two species of crocodiles, the spectral characteristics of their ocular media were also measured. The combined ocular media had a wavelength of 0.5 normalised transmittance at 374–375 nm in both species. The fact that the ocular media absorb a significant proportion of the incident short wavelength light and also that no pigment with a λ_{max} in the ultraviolet region of the visible spectrum was observed in this or other crocodilians (Sillman et al., 1991) suggests that ultraviolet wavelengths do not play a major role in crocodilian visual ecology. Low spectral transmittance at short wavelengths affects the spectral sensitivity function of the SWS single cone in both species and shifts the λ_{max} of the SWS cone 8–9 nm towards longer wavelengths, and will reduce stimulation of the β-peak absorbance band of all other pigments. Because the 50% transmission cut-offs (374 and 375 nm) and transmission curves of the ocular media are very similar in both species, differences in the sensitivity of visual pigments between species are not affected by the spectral transmission of the ocular media. The overall effect of the spectral properties of the ocular media reduces the spectral range of the species and may increase spectral discrimination (Walls and Judd, 1933). Further potential benefits include protection of tissue from the damaging effects of UV rays (Hut et al., 2012) and an increase in visual acuity due to a reduction in the amount of scattered short wavelength light entering the eye (Walls and Judd, 1933). Other ocular components such as the aqueous and vitreous humour and the tapetum lucidum can also affect spectral sensitivity; however, they were not measured in this study. The lack of an ultraviolet sensitive photoreceptor may indicate transmission of a broad range of wavelengths by the aqueous and vitreous humour of both species (as observed in birds; Hart, 2001), while the similar

Journal of Experimental Biology

guanine tapetum observed in the American alligator, *A. mississippiensis*, and the Orinoco crocodile, *C. intermedius*, may suggest similar spectral reflectance across crocodilian species (Laurens and Detwiler, 1921).

Conclusions

The retinal specialisations observed in the saltwater and freshwater crocodile are suitable for a flat environment and provide enhanced sampling for any activities that occur on the surface of the water and at the visual horizon, rendering it useful for conspecific interactions and prey spotting on the riverbank. The similarity in retinal topography and SRP of these two species suggests that the ecological demands on their visual system for detail discrimination tasks are very similar even though the freshwater crocodile is known to hunt smaller animals. This suggests that the ecological pressure on the visual system from prey size preference is not very strong and can be due to small differences in either prey size or eye/body size in juveniles.

The spectral sensitivity differences demonstrate the ability of crocodiles to adapt to subtle differences in photic conditions. Differences in A_1 percentages and the bandwidth of the absorbance curve of the photoreceptors strongly suggest that differences are being driven by a shift in chromophore. They reflect a strong drive to optimise photon catch and may facilitate activities occurring under dim light conditions or unknown social interactions/behaviour that occur underwater. Further studies in the ontogenetic developments and behaviour of crocodiles would elucidate the reason for possessing similar SRPs. In contrast, studying a greater number of species will determine to what extent crocodiles are able to adapt and why other freshwater crocodilians seem to still possess A_1 visual pigments.

Acknowledgements

The authors acknowledge Dr Joao Paulo Coimbra and Dr Yuri Ogawa for scientific advice, encouragement and mentoring.

Competing interests

The authors declare no competing or financial interests.

Author contributions

N.N. designed and conducted experiments and wrote the paper; N.S.H. assisted in experimental design, provided equipment, training and feedback; S.P.C. provided feedback on manuscript; J.M.H. assisted in experimental design and provided feedback.

Funding

Project funding was sourced from an Australian Postgraduate Award (Department of Education and Training, Australian Government) scholarship to N.N., Australian Research Council (ARC) grants to N.S.H. and S.P.C. (DP0558681 and DP1101032394, respectively), a Western Australian Fellowship (Office of Science, Government of Western Australia) to S.P.C. and an ARC Future Fellowship to J.M.H.

References

Abelsdorff, G. (1898). Physiologische Beobachtungen am Auge der Krokodile. *Arch. Anat. Physiol. (Physiol. Abtstr.)*, 155-166.

Ala-Laurila, P., Donner, K. and Koskelainen, A. (2004). Thermal activation and photoactivation of visual pigments. *Biophys. J.* **86**, 3653-3662.

Ala-Laurila, P., Donner, K., Crouch, R. K. and Cornwall, M. C. (2007). Chromophore switch from 11-cis-dehydroretinal (A2) to 11-cis-retinal (A1) decreases dark noise in salamander red rods. *J. Physiol.* **585**, 57-74.

Barbour, H. R., Archer, M. A., Hart, N. S., Thomas, N., Dunlop, S. A., Beazley, L. D. and Shand, J. (2002). Retinal characteristics of the ornate dragon lizard, *Ctenophorus ornatus*. *J. Comp. Neurol.* **450**, 334-344.

Bowmaker, J. K. and Hunt, D. M. (2008). Evolution of vertebrate visual pigments. *Curr. Biol.* **16**, R484-R489.

Brien, M. L., Webb, G. J., Lang, J. W. and Christian, K. A. (2013). Intra- and interspecific agonistic behaviour in hatchling Australian freshwater crocodiles (*Crocodylus johnstoni*) and saltwater crocodiles (*Crocodylus porosus*). *Aust. J. Zool.* **61**, 196-205.

Chen, M., Price, R. M., Yamashita, Y. and Jaffé, R. (2010). Comparative study of dissolved organic matter from groundwater and surface water in the Florida coastal Everglades using multi-dimensional spectrofluorometry combined with multivariate statistics. *Appl. Geochem.* **25**, 872-880.

Chievitz, J. H. (1889). Untersuchungen über die Area centralis retinae. *Arch. Anat. Physiol. Anat. Abt. Suppl.* **13**, 139-196.

Coimbra, J. P., Marceliano, M. L. V., Andrade-da-Costa, B. and Yamada, E. S. (2006). The retina of tyrant flycatchers: topographic organization of neuronal density and size in the ganglion cell layer of the great kiskadee *Pitangus sulphuratus* and the rusty margined flycatcher *Myiozetetes cayanensis* (Aves: Tyrannidae). *Brain Behav. Evol.* **68**, 15-25.

Coimbra, J. P., Trévia, N., Videira Marceliano, M. L., da Silveira Andrade-Da-Costa, B., Picanço-Diniz, C. W. and Yamada, E. S. (2009). Number and distribution of neurons in the retinal ganglion cell layer in relation to foraging behaviors of tyrant flycatchers. *J. Comp. Neurol.* **514**, 66-73.

Coimbra, J. P., Hart, N. S., Collin, S. P. and Manger, P. R. (2013). Scene from above: retinal ganglion cell topography and spatial resolving power in the giraffe (*Giraffa camelopardalis*). *J. Comp. Neurol.* **521**, 2042-2057.

Coimbra, J. P., Collin, S. P. and Hart, N. S. (2014). Topographic specializations in the retinal ganglion cell layer correlate with lateralized visual behavior, ecology, and evolution in cockatoos. *J. Comp. Neurol.* **522**, 3363-3385.

Dartnall, H. J. A. and Lythgoe, J. N. (1965). The spectral clustering of visual pigments. *Vision Res.* **5**, 81-100.

de Busserolles, F., Hart, N. S., Hunt, D. M., Davies, W. I., Marshall, N. J., Clarke, M. W., Hahne, D. and Collin, S. P. (2015). Spectral tuning in the eyes of deep-sea lanternfishes (Myctophidae): a novel sexually dimorphic intra-ocular filter. *Brain Behav. Evol.* **85**, 77-93.

El-Magd, I. A., El Kafrawy, S. and Farag, I. (2014). Detecting oil spill contamination using airborne hyperspectral data in the River Nile, Egypt. *Open J. Mar. Sci.* **4**, 140-150.

Erskine, W. D., Begg, G., Jolly, P., Georges, A., O'Grady, A., Eamus, D., Rea, N., Dostine, P., Townsend, S. Padovan, A. (2003). *Recommended Environmental Water Requirements for the Daly River, Northern Territory, Based on Ecological, Hydrological and Biological Principles*. Technical Report, Vol. 4. Environment Australia.

Fleishman, L. J., Howland, H. C., Howland, M. J., Rand, A. S. and Davenport, M. L. (1988). Crocodiles don't focus underwater. *J. Comp. Physiol. A* **163**, 441-443.

Garrick, L. D. and Lang, J. W. (1977). Social signals and behaviors of adult alligators and crocodiles. *Am. Zool.* **17**, 225-239.

Garten, S. (1907). Die veraenderungen der Netzhaut durch Licht. In *Graefe-Saemisch Handbuch der gesamten Augenheilkunde*, vol. 2 (ed. A. V. Graefe and T. Saemish), pp. 250–280. Leipzig: Springer.

Garza-Gisholt, E., Hemmi, J. M., Hart, N. S. and Collin, S. P. (2014). A comparison of spatial analysis methods for the construction of topographic maps of retinal cell density. *PLoS ONE* **9**, e93485.

Glaser, E. and Wilson, P. (1998). The coefficient of error of optical fractionator population size estimates: a computer simulation comparing three estimators. *J. Microsc.* **192**, 163-171.

Govardovskii, V., Chkheidze, N. and Zueva, L. (1988). Morphofunctional investigation of the retina in the crocodilian caiman *Caiman crocodilus*. *Sens. Syst.* **1**, 19-25.

Govardovskii, V. I., Fyhrquist, N., Reuter, T., Kuzmin, D. G. and Donner, K. (2000). In search of the visual pigment template. *Vis. Neurosci.* **17**, 509-528.

Hall, M. I. (2008). Comparative analysis of the size and shape of the lizard eye. *Zoology* **111**, 62-75.

Hárosi, F. I. (1994). An analysis of two spectral properties of vertebrate visual pigments. *Vision Res.* **34**, 1359-1367.

Hart, N. S. (2001). The visual ecology of avian photoreceptors. *Prog. Retin. Eye Res.* **20**, 675-703.

Hart, N. S. (2004). Microspectrophotometry of visual pigments and oil droplets in a marine bird, the wedge-tailed shearwater *Puffinus pacificus*: topographic variations in photoreceptor spectral characteristics. *J. Exp. Biol.* **207**, 1229-1240.

Hart, N., Partridge, J. and Cuthill, I. (1998). Visual pigments, oil droplets and cone photoreceptor distribution in the European starling (*Sturnus vulgaris*). *J. Exp. Biol.* **201**, 1433-1446.

Hart, N. S., Partridge, J. C. and Cuthill, I. C. (1999). Visual pigments, cone oil droplets, ocular media and predicted spectral sensitivity in the domestic turkey (*Meleagris gallopavo*). *Vision Res.* **39**, 3321-3328.

Hart, N. S., Partridge, J. C., Cuthill, I. C. and Bennett, A. T. D. (2000). Visual pigments, oil droplets, ocular media and cone photoreceptor distribution in two species of passerine bird: the blue tit (*Parus caeruleus* L.) and the blackbird (*Turdus merula* L.). *J. Comp. Physiol. A Sens. Neural Behav. Physiol.* **186**, 375-387.

Hart, N. S., Theiss, S. M., Harahush, B. K. and Collin, S. P. (2011). Microspectrophotometric evidence for cone monochromacy in sharks. *Naturwissenschaften* **98**, 193-201.

Hart, N. S., Coimbra, J. P., Collin, S. P. and Westhoff, G. (2012). Photoreceptor types, visual pigments, and topographic specializations in the retinas of hydrophiid sea snakes. *J. Comp. Neurol.* **520**, 1246-1261.
Hemmi, J. M. and Grünert, U. (1999). Distribution of photoreceptor types in the retina of a marsupial, the tammar wallaby (*Macropus eugenii*). *Vis. Neurosci.* **16**, 291-302.
Hughes, A. (1977). The topography of vision in mammals of contrasting life style: comparative optics and retinal organisation. In *Handbook of Sensory Physiology*, Vol. VII/5 (ed. F. Crescitelli), pp. 613-756. Berlin: Springer-Verlag.
Hut, R. A., Kronfeld-Schor, N., Vinne, V. v. d. and Iglesia, H. D. L. (2012). In search of a temporal niche: environmental factors. In *Progress in Brain Research*, Vol. 199 (ed. A. Kalsbeek, M. Merrow, T. Roenneberg and R. Foster), p. 281. Amsterdam: Elsevier.
Jerlov, N. G. (1976). *Marine Optics*. Amsterdam: Elsevier.
Kay, W. R. (2005). Movements and home ranges of radio-tracked *Crocodylus porosus* in the Cambridge Gulf region of Western Australia. *Wildl. Res.* **31**, 495-508.
Kiltie, R. (2000). Scaling of visual acuity with body size in mammals and birds. *Funct. Ecol.* **14**, 226-234.
Kirk, J. T. O. (1980). Spectral adsorption properties of natural waters: contribution of the soluble and particulate fractions to light absorption in some inland waters of south-eastern Australia. *Mar. Freshw. Res.* **31**, 287-296.
Lang, J. W. (1987). Crocodilian behaviour: implications for management. In *Wildlife Management: Crocodiles and Alligators* (ed. G. J. W. Webb, S. C. Manolis and P. J. Whitehead), pp. 273-294. Sydney: Surrey Beatty and Sons.
Laurens, H. and Detwiler, S. (1921). Studies on the retina. The structure of the retina of *Alligator mississippiensis* and its photomechanical changes. *J. Exp. Zool.* **32**, 207-234.
Levine, J. and MacNichol, E., Jr (1985). Microspectrophotometry of primate photoreceptors: art, artifact and analysis. In *The Visual System* (ed. A. Fein and J. S. Levine), pp. 73-87. New York: Alan R. Liss.
Liebman, P. A. and Granda, A. M. (1971). Microspectrophotometric measurements of visual pigments in two species of turtle, *Pseudemys scripta* and *Chelonia mydas*. *Vision Res.* **11**, 105-114.
Loew, E. R. and Govardovskii, V. I. (2001). Photoreceptors and visual pigments in the red-eared turtle, *Trachemys scripta elegans*. *Vis. Neurosci.* **18**, 753-757.
Lythgoe, J. N. (1972). The adaptation of visual pigments to the photic environment. In *Photochemistry of Vision* (ed. H. J. A. Dartnall), pp. 566-603. Berlin: Springer.
MacNichol, E. F. (1986). A unifying presentation of photopigment spectra. *Vision Res.* **26**, 1543-1556.
Maier, E. J. and Bowmaker, J. K. (1993). Colour vision in the passeriform bird, *Leiothrix lutea*: correlation of visual pigment absorbance and oil droplet transmission with spectral sensitivity. *J. Comp. Physiol. A* **172**, 295-301.
Makaretz, M. and Levine, R. L. (1980). A light microscopic study of the bifoveate retina in the lizard *Anolis carolinensis*: general observations and convergence ratios. *Vision Res.* **20**, 679-686.
Nesbitt, S. J. (2011). The early evolution of archosaurs: relationships and the origin of major clades. *Bull. Am. Mus. Nat. Hist.* **352**, 1-292.
Nychka, D., Furrer, R. and Sain, S. (2015). fields: Tools for Spatial Data. Available at http://CRAN.R-project.org/package=fields.
Oaks, J. R. (2011). A time-calibrated species tree of Crocodylia reveals a recent radiation of the true crocodiles. *Evolution* **65**, 3285-3297.
Parry, J. W. L. and Bowmaker, J. K. (2000). Visual pigment reconstitution in intact goldfish retina using synthetic retinaldehyde isomers. *Vision Res.* **40**, 2241-2247.
Pettigrew, J. D., Dreher, B., Hopkins, C. S., McCall, M. and Brown, M. (1988). Peak density and distribution of ganglion cells in the retinae of microchiropteran bats: implications for visual acuity. *Brain Behav. Evol.* **32**, 39-56.
Pignatelli, V., Champ, C., Marshall, J. and Vorobyev, M. (2010). Double cones are used for colour discrimination in the reef fish, *Rhinecanthus aculeatus*. *Biol. Lett.* **6**, 537-539.
R Development Core Team (2015). *R: A Language and Environment for Statistical Computing*. Vienna, Austria: R Foundation for Statistical Computing.
Richter, A. and Simon, E. (1974). Electrical responses of double cones in the turtle retina. *J. Physiol.* **242**, 673-683.
Röll, B. (2001). Gecko vision: retinal organization, foveae and implications for binocular vision. *Vision Res.* **41**, 2043-2056.
Sillman, A. J., Ronan, S. J. and Loew, E. R. (1991). Histology and microspectrophotometry of the photoreceptors of a crocodilian, *Alligator mississippiensis*. *Proc. R. Soc. B Biol. Sci.* **243**, 93-98.
Slomianka, L. and West, M. J. (2005). Estimators of the precision of stereological estimates: an example based on the CA1 pyramidal cell layer of rats. *Neuroscience* **136**, 757-767.
Snyder, A. W. and Miller, W. H. (1977). Photoreceptor diameter and spacing for highest resolving power. *J. Opt. Soc. Am.* **67**, 696.
Tafani, A. (1883). Parcours et terminaison du nerf optique dans la retine des crocodiles. *Arch. Ital. Biol.* **4**, 210-233.
Taplin, L., Grigg, G. and Beard, L. (1985). Salt gland function in fresh water crocodiles: evidence for a marine phase in eusuchian evolution? In *Biology of Australasian Frogs and Reptiles* (ed. G. Grigg, R. Shine and H. Ehmann), pp. 403-410. Sydney: Surrey Beatty and Sons.
Temple, S. E., Plate, E. M., Ramsden, S., Haimberger, T. J., Roth, W.-M. and Hawryshyn, C. W. (2006). Seasonal cycle in vitamin A1/A2-based visual pigment composition during the life history of coho salmon (*Oncorhynchus kisutch*). *J. Comp. Physiol.* **192**, 301-313.
Temple, S., Hart, N. S., Marshall, N. J. and Collin, S. P. (2010). A spitting image: specializations in archerfish eyes for vision at the interface between air and water. *Proc. R. Soc. B Biol. Sci.* **277**, 2607-2615.
Tucker, A. D., Limpus, C. J., McCallum, H. I. and McDonald, K. R. (1997). Movements and home ranges of *Crocodylus johnstoni* in the Lynd River, Queensland. *Wildl. Res.* **24**, 379-396.
Tucker, A. D., Limpus, C. J., McDonald, K. R. and McCallum, H. I. (2007). Growth dynamics of freshwater crocodiles (*Crocodylus johnstoni*) in the Lynd River, Queensland. *Aust. J. Zool.* **54**, 409-415.
Ueno, Y., Ohba, H., Yamazaki, Y., Tokunaga, F., Narita, K. and Hariyama, T. (2005). Seasonal variation of chromophore composition in the eye of the Japanese dace, *Tribolodon hakonensis*. *J. Comp. Physiol. A* **191**, 1137-1142.
Vorobyev, M., Osorio, D., Bennett, A. T. D., Marshall, N. J. and Cuthill, I. C. (1998). Tetrachromacy, oil droplets and bird plumage colours. *J. Comp. Physiol. A Sens. Neural Behav. Physiol.* **183**, 621-633.
Walls, G. L. (1942). *The Vertebrate Eye and its Adaptive Radiation*. New York: Hafner.
Walls, G. L. and Judd, H. D. (1933). The intra-ocular colour-filters of vertebrates. *Br. J. Ophthalmol.* **17**, 641.
Warrant, E. J. and Nilsson, D.-E. (1998). Absorption of white light in photoreceptors. *Vision Res.* **38**, 195-207.
Webb, G. and Manolis, S. C. (1989). Crocodiles of Australia. Chatswood, NSW: Reed Books.
Webb, G. J. W., Manolis, S. C. and Sack, G. C. (1983). *Crocodylus johnstoni* and *C. porosus* coexisting in a tidal river. *Wildl. Res.* **10**, 639-650.
Webb, G. J. W., Hollis, G. J. and Manolis, S. C. (1991). Feeding, growth, and food conversion rates of wild juvenile saltwater crocodiles (*Crocodylus porosus*). *J. Herpetol.* **25**, 462-473.
West, M. J., Slomianka, L. and Gundersen, H. J. G. (1991). Unbiased stereological estimation of the total number of neurons in the subdivisions of the rat hippocampus using the optical fractionator. *Anat. Rec.* **231**, 482-497.
Whitmore, A. V. and Bowmaker, J. K. (1989). Seasonal variation in cone sensitivity and short-wave absorbing visual pigments in the rudd *Scardinius erythrophthalmus*. *J. Comp. Physiol. A* **166**, 103-115.
Williams, D. R. and Coletta, N. J. (1987). Cone spacing and the visual resolution limit. *J. Opt. Soc. Am. A* **4**, 1514-1523.